

See discussions, stats, and author profiles for this publication at: <https://www.researchgate.net/publication/263978890>

Temperature Stability of Three Commensurate Surface Structures of Coronene Adsorbed on Au(111) from Heptanoic Acid in the 0 to 60 °C Range

ARTICLE *in* THE JOURNAL OF PHYSICAL CHEMISTRY C · JANUARY 2013

Impact Factor: 4.77 · DOI: 10.1021/jp3115435

CITATIONS

14

READS

9

4 AUTHORS, INCLUDING:



Sarah M Vorpahl

University of Washington Seattle

9 PUBLICATIONS 55 CITATIONS

[SEE PROFILE](#)



Ursula Mazur

Washington State University

100 PUBLICATIONS 1,815 CITATIONS

[SEE PROFILE](#)



Kerry W Hipps

Washington State University

167 PUBLICATIONS 5,014 CITATIONS

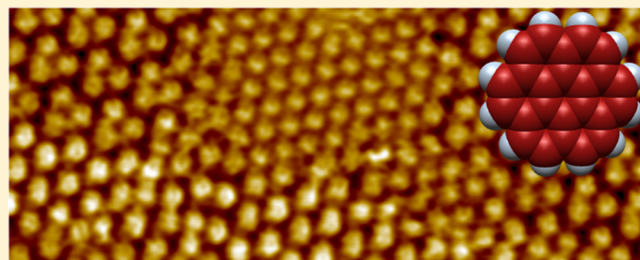
[SEE PROFILE](#)

Temperature Stability of Three Commensurate Surface Structures of Coronene Adsorbed on Au(111) from Heptanoic Acid in the 0 to 60 °C Range

Abdolreza Jahanbekam, Sarah Vorpahl, Ursula Mazur,* and K. W. Hipps*

Department of Chemistry and Materials Science and Engineering Program, Washington State University, Pullman, Washington 99164-4630, United States

ABSTRACT: For the first time, accurate quantitative data on the temperature evolution of a surface monolayer formed at the solution solid interface are reported. In addition, a detailed analysis is provided of the structures of three different monolayers formed when coronene in heptanoic acid is in contact with Au(111). All three monolayer structures are well-defined epitaxial structures that are extremely stable for temperature variations between 0 and 60 °C. At high concentrations, a dense hexagonal structure with molecular separation of 1.19 ± 0.04 nm is observed. At reduced concentration, the most often observed structure is an open hexagonal epitaxial structure with one molecule per unit cell and a molecular separation of 1.45 ± 0.04 nm. This structure is stabilized by solvent molecule adsorption. If the dense phase is exposed to pure solvent, or occasionally with low concentration direct adsorption, then a different hexagonal phase is formed with three molecules per unit cell but exactly the same density (lattice length of 2.46 ± 0.04 nm). Under some conditions, all three phases can be simultaneously present. It is notable that even when the least stable triangular phase is present on a large fraction of the surface, the low-density hexagonal phase is often observed decorating the reconstruction lines. The energy difference between the two low density phases is due to surface–solvent and coronene-adsorbed solvent interactions as the coronene–gold interactions in the two phases are essentially the same. The barrier to thermal conversion between the two low density phases must be several kT or greater than 2 kcal/mol.



INTRODUCTION

The scanning tunneling microscope (STM) has opened the way for detailed molecular level studies of processes at the solution–solid interface. In fact, it is a unique tool for subnanometer level imaging in this environment. Whereas STM imaging studies of the solid–solution interface have been going on for 26 years,¹ studies of the role of solvent, solution concentration, and system temperature have been rare. One of the first concentration studies was reported by Ricci et al.² They demonstrated that molecular packing of stearic acid layers depends on solution concentration. The effect of concentration on the adsorption of thiols on gold has received some attention over the years. Kim and coworkers³ related the adsorption rate of a thiol on gold to the concentration of the thiol in solution. Hobara and coworkers also considered thiols on gold and showed that phase-segregated domains changed with solution concentration.⁴ Kang et al demonstrated a change in thiol monolayer structure as a function of concentration.⁵ Wu and Zhang investigated the replacement of coronene on gold by thiols as a function of thiol solution concentration.⁶

Binary adsorption as a function of concentration has been separately studied by Flynn and coworkers⁷ and by Lackinger's group.⁸ The concentration dependence of the formation of ordered surface structures of acridine-9-carboxylic acid was studied by Xu and coworkers.⁹ Gyarfás and coworkers found

that changing the concentration of coronene in heptanoic acid caused two different surface structures of coronene to form on a Au(111) surface in contact with the solution.¹⁰

There have been even fewer studies on the role of solvent in determining the structure of monolayers of solute molecules at the solution solid interface. Yang and Wang reviewed the literature relating to solvent effects as observed by STM for the period up to 2009.¹¹ Three notable papers prior to 2009 are the studies of Gyarfás,¹⁰ Lackinger,¹² and Tahara.¹³ Gyarfás and coworkers demonstrated that the length of the alkane chain in a series of alkanoic solvents had a role in determining which of two equilibrium structures of coronene on gold was formed. Lackinger demonstrated solvent-dependent polymorphism in trimesic acid self-assembled structures in equilibrium with alkane acids. Tahara and coworkers reported on changes in hexadehydrotribenzo[12]annulene networks formed at the solid–solution interface when aromatic or aliphatic solvents were used. More recently, Takami and coworkers showed that the structure of phthalocyanine complexes on graphite could be manipulated through the choice of solvent.¹⁴

Temperature-dependent studies of systems at the solid–solution interface are also limited.¹⁵ One of the earliest was the

Received: November 22, 2012

Published: January 17, 2013



Giesen and Baier electrochemical STM study of step fluctuations in metal electrodes between 14 and 39 °C.¹⁶ Schull and coworkers studied the diffusion dynamics of different guests in a 2D molecular sieve between −9 and 45 °C.¹⁷ English and Hipps studied the ex situ heating of the Au(111)–coronene–heptanoic acid system up to 105 °C and found new structures that only formed above about 60 °C. Gutzler and coworkers studied 1,3,5-tris(4-carboxyphenyl)-benzene (BTB) adsorbed on HOPG from alkanoic acids between room temperature and 55 °C, in which a transition from a nanoporous low temperature phase to a denser high temperature phase was observed.¹⁸ Marie and coworkers also demonstrated that the density of an adsorbed layer [HBC-C12 on Au(111)] at the solid–solution interface could be adjusted with temperature.¹⁹ Their STM images taken over the 20 to 50 °C range reveal a 2D packing density increase arising from thermally induced desorption of solvent from the gold surface. Most recently, Friesen et al. have controlled both the temperature and oxygen partial pressure to measure the adsorption isotherms and have derived thermodynamic quantities for oxygen binding by cobalt octaethylporphyrin adsorbed on HOPG at the solid–phenyloctane interface.²⁰

In this study, we will explore both the concentration and temperature dependence of the surface structures formed when coronene is adsorbed on Au(111) at the heptanoic acid solution–gold interface. Concentrations ranging between 1×10^{-5} and 3×10^{-6} M were studied between 0 and 60 °C. In addition to the dense and open hexagonal structures previously reported for coronene on gold as a function of concentration, a new trigonal structure is also observed. Carefully calibrated and thermal-drift-corrected images were used to determine lattice parameters for all three structures over the 0 to 60 °C temperature range. All three lattices are found to be commensurate with that of the Au(111) surface, and the orientation of these lattices with respect to the underlying gold structure is also determined. Unlike very few previous studies that reported qualitative observations of structure with temperature, we actually give quantitative lattice spacing as a function of temperature in the 0 to 60 °C range. Second, we show for the first time the existence of a metastable phase with exactly the same surface density as the known low-density hexagonal phase but with three molecules (rather than one) per primitive cell. The existence of this phase poses many interesting questions related to solvent–substrate, solvent–adsorbate, and adsorbate–adsorbate interactions. At the same time, the adsorbate–substrate interactions in the two low density phases are virtually identical, making this system a particularly interesting one for future modeling studies.

■ EXPERIMENTAL SECTION

Coronene (labeled as 97% pure) was purchased from Aldrich and used as supplied. Heptanoic acid was also supplied by Aldrich and was ≥99%. Au(111) films with well-defined terraces were epitaxially grown on mica^{21–23} and were ~0.12 μm thick. The gold films were annealed with a hydrogen flame just prior to use. A stock solution was prepared by adding 0.5 mg of coronene to 10 mL of heptanoic acid in a 10 mL volumetric flask, giving a solution with concentration of 1.7×10^{-4} M. A small magnetic stirring rod was placed in the flask and stirring continued under low heating for 3 to 4 h until all coronene had completely dissolved. Dilute solutions were prepared by using this stock solution. STM samples were fabricated by placing a 15 μL droplet of dilute solution (the

concentration is specified with each image) directly on the gold surface. For specified samples, 15 μL of pure heptanoic acid was added to the surface formed in the previous step. A new piece of gold was used for each day's work.

A Molecular Imaging (now Agilent) Pico-Plus STM was used for all surface images. A high-temperature sample plate (made by Agilent) was used for heating the samples and a Peltier sample plate (Agilent) allowed imaging at temperatures below room temperature. A Lakeshore 321 temperature controller was used with the heating and cooling stages to control temperature to ± 0.1 °C. A current booster (Agilent) was used to augment the Lakeshore output drive in controlling the Peltier sample plate. A gravity-fed ice-water cooling system was used with the Peltier sample plate. Gravity feed was preferred over mechanical pumping because it reduced vibrations.

The microscope was equipped with an environmental chamber that allowed samples to be isolated for imaging in a controlled atmosphere. This chamber also provided acoustic isolation as well as protection from air movement, which can affect image quality. The environmental chamber was especially useful when cooling the sample because purging with nitrogen prevented condensation of water on the sample. After putting the sample into the chamber and before decreasing the temperature, nitrogen gas was flown into the chamber for ~2 h.

Both etched and cut Pt_{0.8}Ir_{0.2} tips were used. Typical settings were adjusted to give a sample bias of −0.7 V, tunneling current near 20 pA, and a scan rate of 4.2 lines/second. All STM images were background-subtracted using SPIP²⁴ image processing software and drift-corrected using a linear drift correction algorithm.^{25,26} The STM was calibrated using the HOPG lattice, and the measured distances were found to have a standard deviation of ± 0.007 nm, whereas the measured angles had a standard deviation of ± 1.9 °. As a result of the coronene lattices being considerably larger than that of graphite (about a factor of 6), it was estimated that the uncertainty in the coronene lattice spacing reported here is ± 0.04 nm.

■ RESULTS AND DISCUSSION

At concentrations of 8×10^{-6} M and higher of coronene in heptanoic acid, the primary structure observed on Au(111) in equilibrium with the solution is a dense hexagonal structure, as seen in Figure 1. The long straight step edges on the Au(111) surface are known to be aligned with the [1,−1,0] direction,^{27,28}

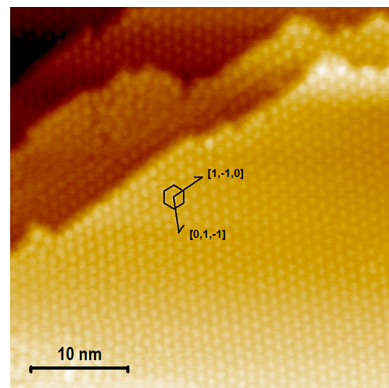


Figure 1. Large area constant current STM image (not drift corrected) of the dense phase formed when coronene 8×10^{-6} M in heptanoic acid is in equilibrium with a Au(111) surface in the temperature interval between 0 and 60 °C.

and the reconstruction lines tend to run perpendicular to that direction,^{28,29} thereby making it easy to assign the orientation of the dense coronene adlayer, as shown in Figure 1. These results are consistent with those of Wu and Zang.⁶ This structure is virtually unchanged between 0 and 60 °C as long as the surface remains in contact with coronene in heptanoic acid solution of at least 8×10^{-6} M. The structure is hexagonal with one molecule per unit cell, and the coronene distances are measured to be 1.19 ± 0.04 nm at all temperatures studied (see Table 1). This structure and concentration range is consistent

Table 1. Molecular Spacing in Nanometers for Coronene Adlayers at the Coronene in Heptanoic Acid Solution Interface with Au(111)^a

temperature	trigonal ^b			
	dense hexagonal	open hexagonal	internal	external
0 °C	1.18	1.45	1.18	2.42
10 °C	1.21		1.19	2.47
20 °C	1.19	1.45	1.19	2.47
40 °C	1.21	1.47	1.20	2.44
60 °C	1.17	1.44	1.20	2.43
average	1.19	1.45	1.19	2.45
epitaxial model ^c	1.15	1.44	1.15	2.50

^a All distances are ± 0.04 nm. ^bFirst distance is the distance between each pair of the three molecules making up the triangles, whereas the external distance is the distance between triangles. The external distance is also the unit cell distance for the hexagonal cell associated with this structure. ^cDistances were calculated assuming that the Au atom separation is 0.288 nm in the Au(111) surface. See the Results and Discussion.

with a previous report by English.³⁰ On the basis of the observed structure and orientation, one can propose an epitaxial relationship between the Au(111) lattice and the dense hexagonal phase. Such a model is presented in Figure 2.

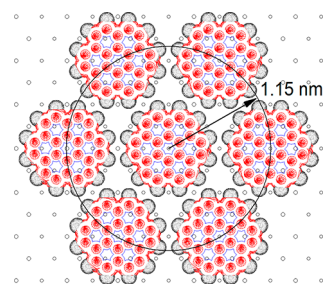


Figure 2. Proposed orientation and structure of the dense hexagonal phase of coronene on Au(111).

Using a value of 0.288 nm for the Au atom spacing,³¹ one then predicts a coronene lattice spacing of 1.15 nm, in good agreement with our experimental value. We note that the location of the gold atom relative to the center of the coronene is unknown, and other orientations are possible. However, this proposed structure seems to us to be the most likely one because it maximizes the Au–C(π) overlap.

If the solution concentration is reduced to 3×10^{-6} M before exposure to a clean Au(111) surface, then a lower density hexagonal structure results (Figure 3). As is the case for the higher density structure, the lattice is primitive hexagonal with one molecule per unit cell and close-packed rows aligned along the [1,−1,0] (and symmetrically equivalent) direction. As in the

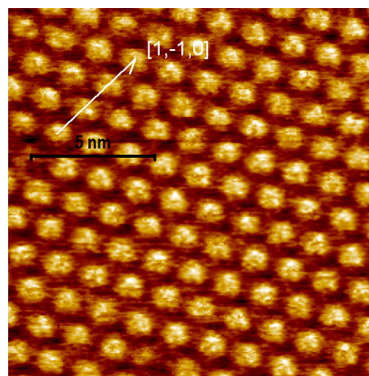


Figure 3. Drift-corrected constant current STM image of the low-density hexagonal phase of coronene on Au(111) formed when in equilibrium with a 3×10^{-6} M solution of coronene in heptanoic acid solution at 60 °C.

dense packing case, this structure is not temperature-dependent and maintains a 1.45 ± 0.04 nm spacing throughout the 0 to 60 °C temperature range, as shown in Table 1. Assuming an epitaxial structure with the observed alignment to the underlying gold, one can propose the lattice relationship presented in Figure 4. In this case, the proposed structure

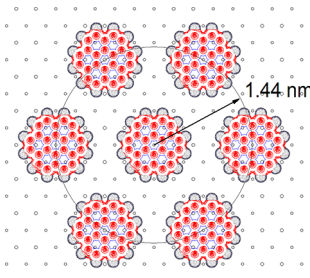


Figure 4. Proposed orientation and structure of the open hexagonal phase of coronene on Au(111).

requires a 1.44 nm coronene spacing, in excellent agreement with our observed structure. As in the dense adlayer case, we drew the structure with an Au atom centered, but other centering is possible.

This open hexagonal structure was previously observed for dilute solution adsorption by Gyarfás¹⁰ and by English.³⁰ They reported lattice spacing of 1.50 ± 0.04 nm based on images that were not drift-corrected, but they did not provide the orientation of the coronene lattice with respect to the Au(111) lattice or the lattice spacing as a function of temperature. Gyarfás and coworkers were able to obtain very high-resolution images at room temperature.¹⁰ They demonstrated that the open hexagonal structure resulted from coadsorption of heptanoic acid with coronene. The heptanoic acid adsorbed in a carboxylate down linear fashion and 12 acid molecules surround each coronene. The hydrogen-bonding network that results from this structure was thought to greatly add to the stability of this low-density structure.¹⁰

Whereas the low-density hexagonal phase is most often observed at lower concentrations, there is a third form that appears with less frequency from very dilute solutions but that is reliably made by first forming the dense phase and then adding pure solvent. This phase has a triangular arrangement of coronene molecules (Figure 5). The internal spacing within the

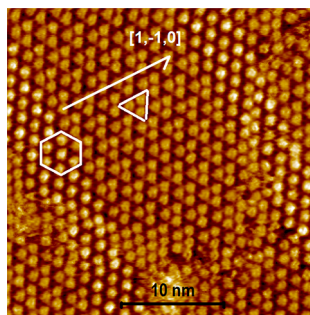


Figure 5. Drift-corrected constant current STM image of the low-density triangular phase of coronene on Au(111) formed when in equilibrium with a heptanoic acid solution between 0 and 60 °C. This sample was first prepared with 1×10^{-5} M coronene in heptanoic acid, and then pure solvent was added.

triangles is the same as in the dense hexagonal phase, but the triangles are spaced more widely apart. The two characteristic spacings are listed as a function of temperature in Table 1, where it is shown that the structure remains the same throughout the studied temperature region. On the basis of the known orientation and spacing, a model for the coronene adlayer as an epitaxial layer was constructed and is displayed in Figure 6, where the distances referenced in Table 1 are also defined. The epitaxial model predicts a coronene separation within a triangle to be 1.15 nm and the separation between triangles to be 2.50 nm, in good agreement with the experimental values of 1.19 ± 0.04 and 2.46 ± 0.04 nm.

Also of note in Figure 5 is the fact that the open hexagonal phase is often the preferred phase on the reconstruction lines of the Au(111) surface. In fact, all three phases are sometimes encountered at the interface between a low concentration solution and the Au(111) surface. An example of such a three-phase region is displayed in Figure 7. The dense hexagonal structure can be seen in the upper middle region of the STM image. The triangular phase is the most prominent, but the low density hexagonal phase can also be seen decorating the

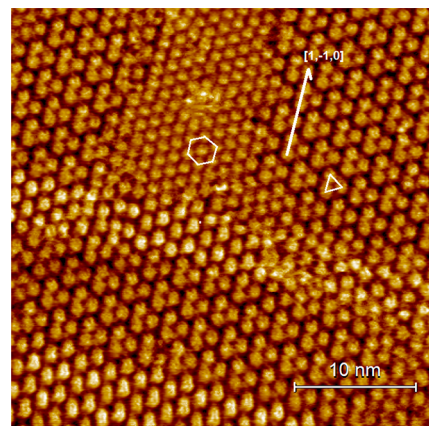


Figure 7. Constant current STM image (not drift corrected) of a three-phase region of coronene on Au(111) in equilibrium with a heptanoic acid solution of coronene. This sample was first prepared with 1×10^{-5} M coronene in heptanoic acid and then pure solvent was added. The bright streaks running through the image are surface reconstruction lines.

reconstruction lines. It should be noted that Figure 7 is not drift-corrected, so there is some distortion in the image. To better understand these phases, we computed the experimental surface density of each phase from the drift-corrected constant current STM images taken from several different samples and imaging regions (Table 2). Whereas there is a 50% increase in

Table 2. Packing Density (molecules/nm²) for the Surface Structures Observed for Coronene in Hepanoic Acid Adsorbed on Au(111) in the Temperature Interval between 0 and 60 °C

	close packed hexagonal	open hexagonal	triangular
average	0.78	0.54	0.53
stand. dev.	0.04	0.02	0.01

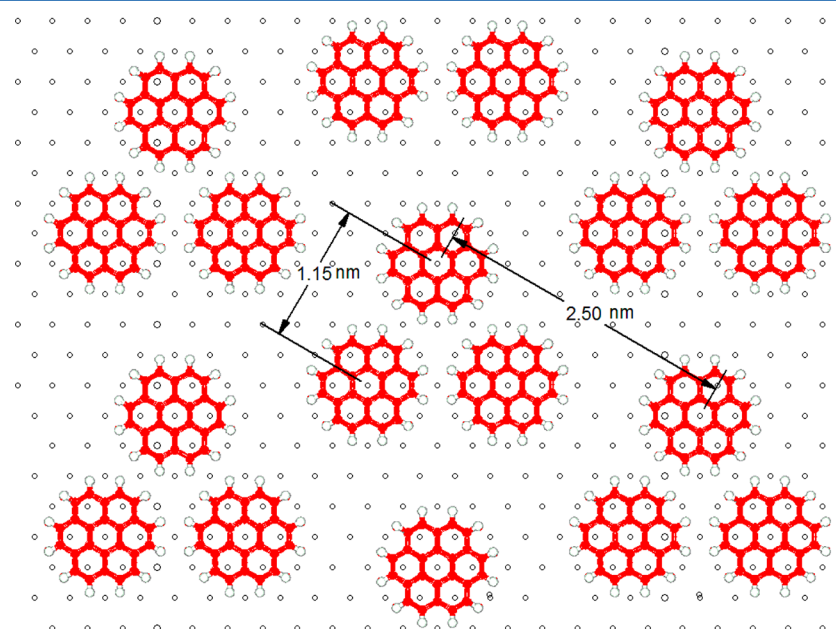


Figure 6. Proposed orientation and structure of the triangular phase of coronene on Au(111).

density in going from the open hexagonal to the dense hexagonal phase, there is no observable change in surface density that results from the conversion between open hexagonal and triangular. The density data suggest that the difference between the low density structures might be imagined as a simple displacement of molecular centers. There are several different pairs of displacement that can connect the two structures, one of which is shown in Figure 8.

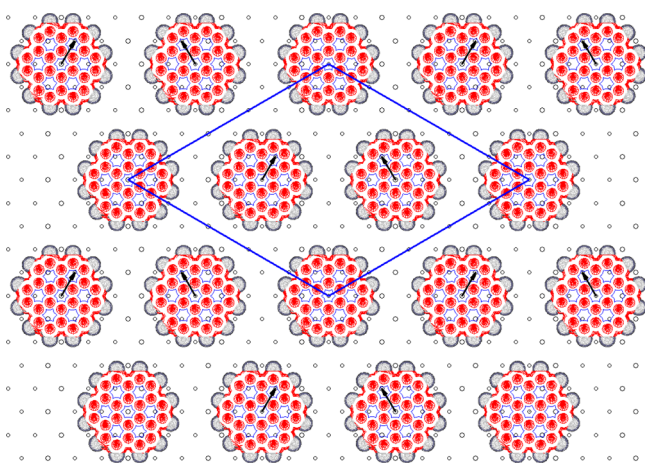


Figure 8. One of several rearrangements that result in an open hexagonal to triangular surface phase conversion. The new hexagonal unit cell (with three molecules per cell) is shown in blue.

In this process (and those related by symmetry), the gold–coronene orientation is unchanged. Thus, the gold–coronene interactions (on the hexagonal portions of the gold surface) are not changing, but the coronene–coronene and surface–solvent interactions are different. The fact that the coronene–coronene and surface–solvent interaction differences are small, or almost cancel, can be seen from the fact that the low density hexagonal structure is present on the surface reconstruction lines simultaneously (and in close proximity) with the triangular structure existing on the hexagonal regions. Also notable in Figure 8 is the fact that the triangular structure is also hexagonal but with three molecules per primitive unit cell (in blue in Figure 8) and this hexagonal unit cell spacing of 2.50 nm. For clarity, we will continue to identify it as the triangular structure rather than the more appropriate “low-density hexagonal phase two”.

Because the coronene–coronene distance in the low density hexagonal phase is too large for significant van der Waals interactions between the coronenes and because the space between the coronene molecules is occupied by carboxylate groups H-bonding with the coronenes, there is a clear van der Waals stabilization of the triangular phase (relative to the low density hexagonal phase), where the coronenes are close-packed within the triangles. Also, the loss of the acid–coronene network of H-bonding seen in the low density hexagonal phase is probably replaced by acid–acid H-bonding on the surface. Exactly how these forces contribute will require a detailed theoretical calculation that is not available now.

Perhaps the most interesting result is that despite the fact that three different structures are stabilized by variation in solvent concentration, sample heating to 60 °C plays little role in determining the structure of the adsorbed phases. Assuming an Arrhenius type dependence, the absence of conversion over a period of many hours suggests that the activation energy is at

least 3RT. Thus, the thermal barrier to interconversion between the two low density phases must be greater than ~2 kcal/mol.

CONCLUSIONS

The monolayer structures formed on Au(111) from solutions of coronene in heptanoic acid are well-defined epitaxial structures that are extremely stable for temperature variations between 0 and 60 °C. At high concentrations, a dense hexagonal structure with molecular separation of 1.19 ± 0.04 nm is observed. At reduced concentration, the most often observed structure is an open hexagonal epitaxial structure with one molecule per unit cell and a molecular separation of 1.45 ± 0.04 nm. This structure is stabilized by solvent molecule adsorption. If the dense phase is exposed to pure solvent, or occasionally with low concentration direct adsorption, then a different hexagonal phase is formed with three molecules per unit cell but exactly the same density (lattice length of 2.46 ± 0.04 nm). The energy difference between the two low density phases is due to surface–solvent and coronene–adsorbed solvent interactions as the coronene–gold interactions in the two phases are essentially the same.

AUTHOR INFORMATION

Corresponding Author

*E-mail: hipps@wsu.edu; Phone: (509) 335-3033 (K.W.H.); E-mail: umazur@wsu.edu; Phone: (509) 335-5822 (U.M.).

Notes

The authors declare no competing financial interest.

ACKNOWLEDGMENTS

This material is based upon work supported by the National Science Foundation under grants CHE-1058435 and CHE-1112156. Instrumentation facilities were supported by a series of NSF grants, the most current being CHE-1048600.

REFERENCES

- (1) Sonnenfeld, R.; Schardt, B. *C. Appl. Phys. Lett.* **1986**, *49*, 1172–1174.
- (2) Ricci, D.; Bonfiglio, A.; Cincotti, S.; Di Zittii, E.; Elementi, L. *Mol. Cryst. Liq. Cryst.* **1993**, *229*, 235–240.
- (3) Kim, D. H.; Noh, J.; Hara, M.; Lee, H. *Bull. Korean Chem. Soc.* **2001**, *22*, 276–80.
- (4) Hobara, D.; Kakiuchi, T. *Electrochem. Commun.* **2001**, *3*, 154–157.
- (5) Kang, H.; Jang, C.; Hara, M.; Noh, J. *J. Nanosci. Nanotechnol.* **2009**, *9*, 7085–7089.
- (6) Wu, S.; Zhang, B. *Langmuir* **2009**, *25*, 1385–1392.
- (7) Yablon, D. G.; Ertas, D.; Fang, H.; Flynn, G. W. *Isr. J. Chem.* **2004**, *43*, 383–392.
- (8) Kampschulte, L.; Werblowsky, T.; Kishore, R.; Schmittel, M.; Heckl, W.; Lackinger, M. *J. Am. Chem. Soc.* **2008**, *130*, 8502–8507.
- (9) Xu, B.; Tao, C.; Williams, E. D.; Reutt-Robey, J. E. *J. Am. Chem. Soc.* **2006**, *128*, 8493–8499.
- (10) Gyarfas, B.; Wiggins, B.; Zosel, M.; Hipps, K. W. *Langmuir* **2005**, *21*, 919–923.
- (11) Yang, Y.; Wang, C. *Curr. Opin. Colloid Interface Sci.* **2009**, *14*, 135–147.
- (12) Lackinger, M.; Gries, S.; Heckl, W.; Hietschold, M.; Flynn, G. W. *Langmuir* **2005**, *21*, 4984–4988.
- (13) Tahara, K.; Furukawa, S.; Uji-i, H.; Uchino, T.; Ichikawa, T.; Zhang, J.; Mamdouh, W.; Sonoda, M.; De Schryver, F.; Feyter, S. D.; Yoshito, T. *J. Am. Chem. Soc.* **2006**, *128*, 16613–16625.
- (14) Takami, T.; Mazur, U.; Hipps, K. W. *J. Phys. Chem. C* **2009**, *113*, 17479–17483.
- (15) MacLeod, J. M.; Rosei, F. *Aust. J. Chem.* **2011**, *64*, 1297–1298.

- (16) Giesen, M.; Baier, S. *J. Phys.: Condens. Matter* **2001**, *13*, 5009–5026.
- (17) Schull, G.; Douillard, L.; Fiorini-Debuisschert, C.; Charra, F.; Mathevet, F.; Kreher, D.; Attias, A. *Adv. Mater.* **2006**, *18*, 2954–57.
- (18) Gutzler, R.; Sirtl, T.; Dienstmaier, J.; Mahata, K.; Heckl, W.; Schmittel, M.; Lackinger, M. *J. Am. Chem. Soc.* **2010**, *132*, 5084–5090.
- (19) Marie, C.; Silly, F.; Tortech, L.; Mullen, K.; Fichou, D. *ACS Nano* **2010**, *4*, 1288–1292.
- (20) Friesen, B. A.; Bhattacharai, A.; Mazur, U.; Hipps, K. W. *J. Am. Chem. Soc.* **2012**, *134*, 14897–14904.
- (21) Lu, X.; Hipps, K. W. *J. Phys. Chem. B* **1997**, *101*, 5391–5396.
- (22) Lu, X.; Hipps, K. W.; Wang, X.; Mazur, U. *J. Am. Chem. Soc.* **1996**, *118*, 7197–7202.
- (23) Barlow, D.; Hipps, K. W. *J. Phys. Chem. B* **2000**, *104*, 5993–6000.
- (24) SPIP is a product of Image Metrology, Lyngsø Alle 3A, DK-2970 Hørsholm, Denmark.
- (25) Tong, W.; Xue, Y.; Zimmt, M. B. *J. Phys. Chem. C* **2010**, *114*, 20783–20792.
- (26) Tong, W. Controlling Self-Assembled Monolayer Morphology with Dipolar Interactions: Preparation, STM Image Analysis and Simulations of 1,5-(Disubstituted)-Anthracene Monolayers. Ph.D. Thesis, Brown University, Providence, RI, 2010.
- (27) Zhang, L.; Cheng, Z.; Huan, Q.; He, X.; Lin, X.; Gao, L.; Deng, Z.; Jiang, N.; Liu, Q.; Du, S.; Guo, H.; Gao, H. *J. Phys. Chem. C* **2011**, *115*, 10781–10796.
- (28) Repan, V.; Berrior, J. M.; Rousset, S.; Lecoeur. *J. Applied Surf. Sci.* **2000**, *162–163*, 30–36.
- (29) Barth, J. V.; Brune, H.; Ertl, G.; Behm, R. *J. Phys. Rev. B* **1990**, *42*, 9307–9318.
- (30) English, W.; Hipps, K. W. *J. Phys. Chem. C* **2008**, *112*, 2026–2031.
- (31) Maeland, A.; Flanagan, T. B. *Can. J. Phys.* **1964**, *42*, 2364–2366.